

Numerical study of duality and universality in a frozen superconductor

T. Neuhaus,^{1,*} A. Rajantie,^{2,3,†} and K. Rummukainen^{4,5,‡}

¹*Finkenweg 15, D-33824 Werther, Germany*

²*DAMTP, CMS, University of Cambridge, Cambridge CB3 0WA, United Kingdom*

³*Institute for Theoretical Physics, University of California, Santa Barbara, CA 93106, USA*

⁴*NORDITA, Blegdamsvej 17, DK-2100 Copenhagen Ø, Denmark*

⁵*Department of Physics, P.O.Box 64, FIN-00014 University of Helsinki, Finland*

(Dated: 24 May, 2002)

The three-dimensional integer-valued lattice gauge theory, which is also known as a “frozen superconductor,” can be obtained as a certain limit of the Ginzburg-Landau theory of superconductivity, and is believed to be in the same universality class. It is also exactly dual to the three-dimensional XY model. We use this duality to demonstrate the practicality of recently developed methods for studying topological defects, and investigate the critical behaviour of the phase transition using numerical Monte Carlo simulations of both theories. On the gauge theory side, we concentrate on the vortex tension and the penetration depth, which map onto the correlation lengths of the order parameter and the Noether current in the XY model, respectively. We show how these quantities behave near the critical point, and that the penetration depth exhibits critical scaling only very close to the transition point. This may explain the failure of superconductor experiments to see the inverted XY model scaling.

PACS numbers: 74.60.-w, 64.60.Cn, 64.60.Fr, 11.15.Ha

I. INTRODUCTION

Duality arguments suggest that the superconductor-insulator phase transition should be in the same universality class as the three-dimensional XY model, but with an inverted temperature axis.^{1,2,3,4,5} This means that the superconducting phase maps onto the symmetric phase, and the normal phase onto the broken phase. Furthermore, the dual counterpart of the order parameter of the XY model is a non-perturbative field that creates the Abrikosov-Nielsen-Olesen vortices in the superconductor.

The most direct prediction of the duality is that the critical magnetic field H_{c1} , or equivalently the vortex tension \mathcal{T} , should scale with the XY model critical exponent $\nu_{XY} \approx 0.6723$.⁶ In practice, it is easier to measure the scaling exponent ν' of the penetration depth λ , but for that quantity, the theoretical picture is less clear. Both $\nu' \approx 0.33$ ⁷ and $\nu' \approx 0.5$ ^{4,5} were suggested before the prediction eventually converged to $\nu' = \nu_{XY}$.⁸

Ironically, two different experiments with $\text{YBa}_2\text{Cu}_3\text{O}_{7-\delta}$ high-temperature superconductor have produced results that are each compatible with one of the earlier suggestions, namely $\nu' = 0.34(1)$,⁹ and $\nu' = 0.45 \dots 0.5$.¹⁰

Similarly, it has turned out to be difficult to confirm the duality in Monte Carlo simulations of the Ginzburg-Landau theory away from the London limit,¹¹ as they also seem to favour $\nu' \approx 0.3$. In the London limit, where the duality is on a firmer footing,^{12,13} simulations^{14,15} give $\nu' \approx 0.67$ through indirect measurements, though.

There are two principal reasons for all this confusion:

1. The duality relation is expected to apply quantitatively only in a narrow temperature interval near the critical point, where the vortex tension/ $k_B T$

is well below the inverse correlation lengths of the scalar and photon fields.

2. The duality relates the fundamental fields and thermodynamical densities of one theory to non-perturbative and non-local objects in the other. These are difficult to measure both in experiments and in numerical simulations.

In the London limit, the difficulty (1) is alleviated, as the scalar correlation length is very short, but in this paper we go even further and take another limit to obtain the Abelian integer-valued lattice gauge theory, “frozen superconductor” (FZS).¹ For this theory, the duality transformation can be carried out exactly, and yields precisely the three-dimensional XY model with the Villain action.^{1,12,16,17} The duality is therefore exactly valid at all temperatures.

The FZS does not have a scalar (Higgs) field to drive the transition, but it still has a transition between a low-temperature superconducting phase with massive gauge field excitations, and a high-temperature massless phase. (Microscopically, this transition is due to the “freezing” of the discrete gauge variables below the critical temperature; hence the name frozen superconductor.) This is mapped to the symmetry breaking transition of the XY-Villain model, with inverted temperature ($T \leftrightarrow 1/T$). Since the duality is valid at all temperatures, the problem (1) above is completely avoided.

In this paper we study the duality relation in detail with lattice Monte Carlo simulations. Our aim is *not* to numerically verify the duality — it is, after all, a mathematical identity. Rather, the purpose is to identify “good” observables and possible pitfalls in Monte Carlo studies of the duality relations of this type, especially bearing in mind the problems encountered in the

Ginzburg-Landau theory simulations. In this way, we hope to find out how to avoid the difficulty (2) in more realistic cases.

The main body of the paper is concerned with the calculation of gauge invariant (non-local) order parameters of the FZS; the vortex tension \mathcal{T} , the photon mass m_γ and the magnetic permeability χ_m . We relate these observables to their duals in the XY model, and study the critical behaviour.

This paper is organized as follows. Section II contains the definition of the two models and discusses the duality between them. Section III introduces the observables and Section IV discusses their qualitative behaviour in the two phases. In Section V, the location of critical point is determined using the spin correlator in the XY model, and Section VI deals with the definition and the measurement of its dual counterpart, the vortex tension. In Section VII we study the susceptibilities, i.e., the photon correlator in the momentum space, and discuss the mass determination from them, and in Section VIII, we extract the photon mass directly from the exponential decay of the correlation function in the coordinate space. Finally, Section IX lists the main findings and concludes the paper.

II. DUALITY

We start by formulating the three-dimensional Ginzburg-Landau (GL) theory in the London limit on a three-dimensional cubic lattice. The theory consists of a real valued gauge field $A_{\mathbf{x},i}$ defined on links and spin angles $\theta_{\mathbf{x}}$ defined on lattice sites. The partition function is

$$Z_{\text{GL}} = \int \left(\prod_{\mathbf{x}} d\theta_{\mathbf{x}} \prod_i dA_{\mathbf{x},i} \right) \exp \left(- \sum_{\mathbf{x}} \mathcal{L}_{\text{GL},\mathbf{x}} \right), \quad (1)$$

where

$$\mathcal{L}_{\text{GL},\mathbf{x}} = \frac{1}{2} \sum_{i < j} F_{\mathbf{x},ij}^2 + \kappa \sum_i s(\theta_{\mathbf{x}+i} - \theta_{\mathbf{x}} - qA_{\mathbf{x},i}), \quad (2)$$

We shall now show that the partition functions (5) and (7) are dual to each other, i.e., proportional to each other if $\beta = 1/\kappa$. Introducing a real vector field $h_{\mathbf{x},i}$,¹⁹ we can write Eq. (7) as

$$Z_{\text{XY}}(\kappa) \propto \int D\theta D h_i \sum_{k_i} \exp \left[- \sum_{\mathbf{x},i} \left(\frac{1}{2\kappa} h_{\mathbf{x},i}^2 - i h_{\mathbf{x},i} \Delta_{\mathbf{x},i}^{\text{XY}} \right) \right], \quad (8)$$

where we have introduced the Noether current of the XY model

$$\Delta_{\mathbf{x},i}^{\text{XY}} = \theta_{\mathbf{x}+i} - \theta_{\mathbf{x}} - 2\pi k_{\mathbf{x},i}. \quad (9)$$

The integration over θ yields a delta function $\delta(\nabla \cdot \mathbf{h})$, where we have defined the lattice divergence

$$\nabla \cdot \mathbf{h}_{\mathbf{x}} = \sum_i (h_{\mathbf{x},i} - h_{\mathbf{x}-i,i}). \quad (10)$$

and

$$F_{\mathbf{x},ij} = A_{\mathbf{x},i} + A_{\mathbf{x}+i,j} - A_{\mathbf{x}+j,i} - A_{\mathbf{x},j}, \quad (3)$$

and $s(x)$ is a periodic function with period 2π and minimum at $x = 0$. The standard choice for $s(x)$ is $s(x) = -\cos(x)$, but here we shall use the Villain form¹⁸

$$s(x) = -\ln \sum_{k=-\infty}^{\infty} \exp \left(-\frac{1}{2}(x - 2\pi k)^2 \right). \quad (4)$$

In this paper we shall consider two limits of this theory. The frozen superconductor (FZS),^{1,12} which we also refer to as simply “the gauge theory,” is obtained by taking $\kappa \rightarrow \infty$ and defining $\beta = 4\pi^2/q^2$. This leads to the partition function

$$Z_{\text{FZS}}(\beta) = \sum_{\{I_{\mathbf{x},i}\}} \exp \left(-\frac{\beta}{2} \sum_{\mathbf{x},i>j} P_{\mathbf{x},ij}^2 \right), \quad (5)$$

where

$$P_{\mathbf{x},ij} = I_{\mathbf{x},i} + I_{\mathbf{x}+i,j} - I_{\mathbf{x}+j,i} - I_{\mathbf{x},j}, \quad (6)$$

and the link variables $I_{\mathbf{x},i} = qA_{\mathbf{x},i}/2\pi$ take integer values. This model has two phases: the Coulomb phase ($\beta < \beta_c$) and the superconducting phase ($\beta > \beta_c$).

We also consider the limit $q \rightarrow 0$, in which we recover the three-dimensional XY model. The gauge field $A_{\mathbf{x},i}$ decouples, and the non-trivial spin part of the partition function becomes

$$Z_{\text{XY}}(\kappa) = \int D\theta \exp \left(-\kappa \sum_{\mathbf{x},i} s(\theta_{\mathbf{x}+i} - \theta_{\mathbf{x}}) \right). \quad (7)$$

This model has a broken phase at $\kappa > \kappa_c$ and a symmetric phase at $\kappa < \kappa_c$.

The summation over $k_{\mathbf{x},i}$ restricts $h_{\mathbf{x},i}$ to integer values, and we obtain¹⁶

$$Z_{XY}(\kappa) \propto \sum_{\{h\}} \delta_{\nabla \cdot \mathbf{h}, 0} \exp \left(-\frac{1}{2\kappa} \sum_{\mathbf{x},i} h_{\mathbf{x},i}^2 \right), \quad (11)$$

which is the partition function of an integer-valued and sourceless vector field. In an infinite volume, we can interpret the vector field $h_{\mathbf{x},i}$ as the integer valued flux through the dual lattice plaquette pierced by link (\mathbf{x}, i) , and write

$$h_{\mathbf{x},i} = \frac{1}{2} \epsilon_{ijk} P_{\mathbf{x},jk}, \quad (12)$$

with $P_{\mathbf{x},jk}$ as in Eq. (6).

Thus, identifying $\beta = 1/\kappa$, we recover the partition function in Eq. (5).^{1,12,17} This shows that the two limits of Eq. (1), $\kappa \rightarrow \infty$ and $q \rightarrow 0$, are dual to each other. In particular, the duality relation implies that the gauge theory has a phase transition of the XY model universality class at $\beta_c = 1/\kappa_c$, and the Coulomb and superconducting phases are mapped to the broken and symmetric phases, respectively. Note, however, that duality only maps the two limits onto each other; the Ginzburg-Landau theory is not self-dual for finite parameter values.

The nature of the duality transformation becomes more transparent when we introduce an external, real-valued vector field $\alpha_{\mathbf{x},i}$ in the XY model

$$Z_{XY}(\kappa; \{\alpha_{\mathbf{x},i}\}) = \int D\theta \sum_{\{k_{\mathbf{x},i}\}} \exp \left[-\sum_{\mathbf{x},i} \left(\frac{\kappa}{2} (\Delta_{\mathbf{x},i}^{XY})^2 + i\alpha_{\mathbf{x},i} \Delta_{\mathbf{x},i}^{XY} \right) \right]. \quad (13)$$

Introducing $h_{\mathbf{x},i}$ as in Eq. (8), but defining $\tilde{h}_{\mathbf{x},i} = h_{\mathbf{x},i} - \alpha_{\mathbf{x},i}$, we obtain

$$Z_{XY}(\kappa; \{\alpha_{\mathbf{x},i}\}) \propto \int D\theta D\tilde{h}_i \sum_{k_i} \exp \left[-\sum_{\mathbf{x},i} \left(\frac{1}{2\kappa} (\tilde{h}_{\mathbf{x},i} + \alpha_{\mathbf{x},i})^2 - i\tilde{h}_{\mathbf{x},i} \Delta_{\mathbf{x},i}^{XY} \right) \right]. \quad (14)$$

Now, as before, we integrate over $\theta_{\mathbf{x}}$, which constrains $\nabla \cdot \tilde{\mathbf{h}}_{\mathbf{x}} = 0$, sum over $k_{\mathbf{x},i}$, which makes $\tilde{h}_{\mathbf{x},i}$ an integer, and express $\tilde{h}_{\mathbf{x},i}$ in terms of $P_{\mathbf{x},ij}$ as in Eq. (12). This gives us

$$Z_{XY}(\kappa; \{\alpha_{\mathbf{x},i}\}) = Z_{\text{FZS}}(1/\kappa; \{\alpha_{\mathbf{x},i}\}), \quad (15)$$

where

$$Z_{\text{FZS}}(\beta; \{\alpha_{\mathbf{x},i}\}) = \sum_{\{I_{\mathbf{x},i}\}} \exp \left[-\frac{\beta}{2} \sum_{\mathbf{x},i} \left(\frac{1}{2} \epsilon_{ijk} P_{\mathbf{x},jk} + \alpha_{\mathbf{x},i} \right)^2 \right], \quad (16)$$

Note that in this expression the vector field α is defined on the dual lattice, i.e. $\alpha_{\mathbf{x},i}$ lives on the link that pierces the plaquette $P_{\mathbf{x},jk}$. Eq. (15) is the basic duality equation, which can be used to relate the observables of the two models to each other.

III. OBSERVABLES

A. Spin-spin correlator

The basic observable in the XY model is the spin-spin correlation function,

$$G_{\mathbf{x}_1, \mathbf{x}_2} \equiv \langle \exp[i(\theta_{\mathbf{x}_1} - \theta_{\mathbf{x}_2})] \rangle_{XY}. \quad (17)$$

Using Eq. (13), we can write this as

$$G_{\mathbf{x}_1, \mathbf{x}_2} = \frac{Z_{XY}(\kappa; \{\alpha_{\mathbf{x},i}\})}{Z_{XY}(\kappa)}, \quad (18)$$

where $\alpha_{\mathbf{x},i}$ is an otherwise arbitrary fixed integer-valued vector field, but it satisfies the condition

$$\nabla \cdot \alpha = \delta_{\mathbf{x}, \mathbf{x}_1} - \delta_{\mathbf{x}, \mathbf{x}_2}, \quad (19)$$

i.e. it has a source and a ‘‘sink’’ at points \mathbf{x}_1 and \mathbf{x}_2 , respectively.

The duality relation in Eq. (15) implies that Eq. (18) must be equal to

$$G_{\mathbf{x}_1, \mathbf{x}_2} = \left\langle \exp \left(-\frac{\beta}{2} \sum_{\mathbf{x},i} (\epsilon_{ijk} \alpha_{\mathbf{x},i} P_{\mathbf{x},jk} + \alpha_{\mathbf{x},i}^2) \right) \right\rangle_{\text{FZS}}. \quad (20)$$

The simplest choice for $\alpha_{\mathbf{x},i}$ vanishes everywhere except on the shortest path of links that leads from \mathbf{x}_1 to \mathbf{x}_2 , on which it has the value of unity. As we shall see later in Sec. VI, Eq. (20) then has a natural interpretation as a vortex correlation function in the gauge theory.^{1,16,20}

In the symmetric phase of the XY model, i.e., when $\kappa < \kappa_c$, the spin-spin correlator decays exponentially as

$$G_{\mathbf{x}_1, \mathbf{x}_2} \propto e^{-m|\mathbf{x}_1 - \mathbf{x}_2|}, \quad (21)$$

where we call the decay rate m the scalar mass, in accordance with a field theory picture. By definition, the correlation length is given by its inverse $\xi = 1/m$. Eq. (20) implies that under the duality transformation, the scalar mass becomes the vortex tension defined in Sec. VI, $\mathcal{T} = m$.

In the broken phase of the XY model, where $\kappa > \kappa_c$, the spin-spin correlator (17) approaches a constant

$$\lim_{|\mathbf{x}_1 - \mathbf{x}_2| \rightarrow \infty} G_{\mathbf{x}_1, \mathbf{x}_2} = M^2, \quad (22)$$

where M is the magnetization.

More generally one can also consider higher n -point functions in the XY model, which correspond to external fields $\alpha_{\mathbf{x},i}$ with more sources and sinks.

We would like to emphasize the difference between our approach and the attempts to describe the phase transition of the XY model as vortex percolation.^{21,22,23} The ‘‘line tension’’ discussed in that context is defined using the length distribution of vortices in the XY model and suffers from certain ambiguities, and there is numerical evidence that the percolation point at which the line tension vanishes does not even coincide with the thermodynamic critical point κ_c .²⁴ In contrast, our \mathcal{T} is the vortex tension in the gauge theory, is a well-defined, unambiguous observable and, due to the exact nature of the duality, reflects the true thermodynamic properties of the system.

B. Helicity modulus

Another important quantity in the XY model is the helicity modulus,²⁵ which characterizes the response of the free energy to a twist of the spins by an amount $\delta\theta$ along, say, the z direction. Instead of period boundary conditions for θ , we would instead have $\theta(x, y, z + N) = \theta(x, y, z) + \delta\theta$. It is convenient to define a periodic variable

$$\tilde{\theta}(x, y, z) = \theta(x, y, z) - \frac{z}{N}\delta\theta \equiv \theta(x, y, z) - zj_3, \quad (23)$$

where $j_3 = \delta\theta/N$ is the average Noether current created by the twist. We can then write the twisted partition function as

$$Z_{\text{XY}}(\kappa, j_i) = \int D\theta \sum_{\{k_{\mathbf{x},i}\}} \exp \left[- \sum_{\mathbf{x},i} \left(\frac{\kappa}{2} (\Delta_{\mathbf{x},i}^{\text{XY}} + j_i)^2 \right) \right], \quad (24)$$

where $\mathbf{j} = (0, 0, j_3)$.

The helicity modulus is defined as

$$\Upsilon = \frac{N_3}{N_1 N_2} \left(\frac{\partial^2 F}{\partial \delta \theta^2} \right)_{\delta \theta = 0} = \frac{1}{V} \left(\frac{\partial^2 F}{\partial j_3^2} \right)_{j_3 = 0}, \quad (25)$$

where $F = -\ln Z_{\text{XY}}$ is the free energy of the system. It is an order parameter, with finite, non-zero values $\Upsilon > 0$ in the broken phase ($\kappa > \kappa_c$) and a vanishing value $\Upsilon = 0$ in the symmetric phase ($\kappa < \kappa_c$). If the XY model is viewed as a model for a superfluid, Υ is proportional to the superfluid density, $\Upsilon \propto \rho_s$. We can also write Υ as

$$\begin{aligned} \Upsilon &= -\frac{1}{V} \frac{1}{Z_{\text{XY}}} \frac{\partial^2 Z_{\text{XY}}}{\partial j_3^2} = -\frac{\kappa}{V} \left[\kappa \left\langle \left(\sum_{\mathbf{x}} \Delta_{\mathbf{x},3}^{\text{XY}} \right)^2 \right\rangle - V \right] \\ &= \kappa (1 - \kappa \chi), \end{aligned} \quad (26)$$

where $\chi = \sum_{\mathbf{x}} \langle \Delta_{\mathbf{0},3}^{\text{XY}} \Delta_{\mathbf{x},3}^{\text{XY}} \rangle$ is a susceptibility related to the U(1) current density of the XY model.

It is interesting to ask what the helicity modulus Υ corresponds to in the gauge theory. Formally, it is related to Eq. (13) with a constant imaginary field $\alpha_i = -i\kappa j_i$,

$$Z_{\text{XY}}(\kappa, j_i) = Z_{\text{XY}}(\kappa; \{\alpha_i\}) \exp \left(-\frac{\kappa}{2} V j_i^2 \right), \quad (27)$$

and therefore

$$\Upsilon = \frac{\kappa^2}{V} \frac{1}{Z_{\text{XY}}} \frac{\partial^2 Z_{\text{XY}}}{\partial \alpha_3^2} + \kappa = \frac{1}{\beta^2 V} \frac{1}{Z_{\text{FZS}}} \frac{\partial^2 Z_{\text{FZS}}}{\partial \alpha_3^2} + \frac{1}{\beta}. \quad (28)$$

Using Eq. (5), this is nothing but

$$\Upsilon = \frac{1}{V} \left\langle \left(\sum_{\mathbf{x}} P_{\mathbf{x},12} \right)^2 \right\rangle \equiv \chi_m, \quad (29)$$

where we have defined the magnetic permeability χ_m as the susceptibility associated with the magnetic flux in the FZS.

C. Photon mass

From the FZS point of view, the most natural observable is the photon correlator, defined as the correlation function of plaquettes,

$$\Gamma_{(\mathbf{x}_1, i)(\mathbf{x}_2, j)} = \langle P_{\mathbf{x}_1, kl} P_{\mathbf{x}_2, mn} \rangle_{\text{FZS}} \quad (ikl \text{ and } jmn \text{ cyclic}) \quad (30)$$

In the superconducting phase ($\beta > \beta_c$), this correlator decays exponentially, and we call the decay rate the photon mass m_γ . The penetration depth λ is defined as the inverse of the photon mass, $\lambda = 1/m_\gamma$. In the non-superconducting Coulomb phase ($\beta < \beta_c$), $\Gamma_{(\mathbf{x}_1, i)(\mathbf{x}_2, j)}$ has a power-law decay, which corresponds to vanishing photon mass $m_\gamma = 0$, or infinite penetration depth $\lambda = \infty$.

	XY model	FZS	
spin-spin correlator	$G_{\mathbf{x}_1, \mathbf{x}_2}$	Eq. (20)	vortex correlator
scalar mass	$m = 1/\xi$	\mathcal{T}	vortex tension
helicity modulus	Υ	χ_m	magnetic permeability
current-current correlator	$-\beta^{-2} \langle \Delta_{\mathbf{x}_1, i}^{\text{XY}} \Delta_{\mathbf{x}_2, j}^{\text{XY}} \rangle$	$\Gamma_{(\mathbf{x}_1, i)(\mathbf{x}_2, j)}$	photon correlator

TABLE I: Comparison of the basic observables in the XY model and in the frozen superconductor (FZS).

We write the photon correlation function as

$$\Gamma_{(\mathbf{x}_1, i)(\mathbf{x}_2, j)} = \frac{1}{\beta^2 Z_{\text{FZS}}(\beta)} \left. \frac{\partial^2 Z_{\text{FZS}}(\beta; \{\alpha_{\mathbf{x}, i}\})}{\partial \alpha_{\mathbf{x}_1, i} \partial \alpha_{\mathbf{x}_2, j}} \right|_{\alpha=0}, \quad (31)$$

which is simply a generalization of Eq. (28) to a non-constant $\alpha_{\mathbf{x}, i}$. Using the duality (15), we find

$$\Gamma_{(\mathbf{x}, i)(\mathbf{y}, j)} = \frac{1}{\beta} \delta_{\mathbf{x}, \mathbf{y}} \delta_{ij} - \frac{1}{\beta^2} \langle \Delta_{\mathbf{x}, i}^{\text{XY}} \Delta_{\mathbf{y}, j}^{\text{XY}} \rangle_{\text{XY}}. \quad (32)$$

In practice, it is more convenient to study correlations between planes rather than individual plaquettes. To this end, we interpret the z direction as “time” and label it with τ . We consider the photon correlation function with a non-zero “spatial” momentum $\underline{\mathbf{p}}$, where we use the underline to indicate a two-vector in the $(1, 2)$ plane. (The zero-momentum correlation function vanishes identically.) The correlation function is defined as

$$\Gamma(\tau, \underline{\mathbf{p}}) = \frac{1}{N_3} \text{Re} \left\{ \sum_{\tau_0} \sum_{\underline{\mathbf{x}}, \underline{\mathbf{y}}} \langle P_{\mathbf{x}, 12} P_{\mathbf{y}, 12} \rangle e^{-i\underline{\mathbf{p}} \cdot (\underline{\mathbf{x}} - \underline{\mathbf{y}})} \right\}, \quad (33)$$

where $p_i = 2\pi k_i / N_i$, ($i = 1, 2$) and k_i are integers, $\mathbf{x} = (\tau_0, \underline{\mathbf{x}})$ and $\mathbf{y} = (\tau_0 + \tau, \underline{\mathbf{y}})$.

It is also useful to consider the three-dimensional Fourier transform of the photon correlator

$$\Gamma_{ij}(\mathbf{p}) = \sum_{\mathbf{x}} e^{-i\mathbf{p} \cdot \mathbf{x}} \Gamma_{(0, i)(\mathbf{x}, j)}. \quad (34)$$

Eq. (32) then translates into

$$\Gamma_{ij}(\mathbf{p}) = \frac{1}{\beta} \delta_{ij} - \frac{1}{\beta^2} \langle \Delta_i^{\text{XY}}(-\mathbf{p}) \Delta_j^{\text{XY}}(\mathbf{p}) \rangle_{\text{XY}}. \quad (35)$$

Note that

$$\chi_m = \lim_{\mathbf{p} \rightarrow 0} \Gamma_{33}(\mathbf{p}). \quad (36)$$

More generally, we can see that there is a direct correspondence between the photon in the gauge theory and the Noether current density $\Delta_{\mathbf{x}, i}^{\text{XY}}$ in the XY model.

IV. PHASE STRUCTURE

A. Symmetric/superconducting phase

In the XY model, the symmetric phase ($\kappa < \kappa_c$) is characterized by vanishing magnetization M and a finite

correlation length $\xi = 1/m$. The helicity modulus Υ is zero, and therefore Eq. (26) implies that $\chi = 1/\kappa$. When the critical point is approached, the correlation length ξ diverges as $\xi \sim |\kappa - \kappa_c|^{-\nu}$. Numerical studies [using the cosine action rather than Eq. (4)] have shown that $\nu \approx 0.6723$.⁶

In the FZS, this corresponds to the superconducting phase ($\beta > \beta_c$). The above implies that the vortex tension \mathcal{T} , which is equal to the scalar mass $m = 1/\xi$ of the XY model, is non-zero, and vanishes as $\mathcal{T} \sim |\beta - \beta_c|^\nu$ at the transition point.

The magnetic permeability χ_m , which is equal to Υ vanishes everywhere in the superconducting phase. However, we can define the gauge field susceptibility χ_A by [cf. Eq. (36)]

$$\chi_A = \lim_{\underline{\mathbf{p}} \rightarrow 0} \frac{\Gamma_{33}(\underline{\mathbf{p}})}{\underline{\mathbf{p}}^2}, \quad (37)$$

where the underline indicates that $\underline{\mathbf{p}}$ is a two-vector in the $(1, 2)$ plane. This quantity diverges as the critical point is approached, and we parameterize this divergence by the exponent γ_A ,

$$\chi_A \sim |\beta - \beta_c|^{-\gamma_A}. \quad (38)$$

It was argued in Ref. 14 that $\gamma_A = \nu$.

The photon correlator $\Gamma_{(\mathbf{x}_1, i)(\mathbf{x}_2, j)}$ decays exponentially in this phase, and the penetration depth λ is therefore finite. It diverges at the transition point as $\lambda \sim |\beta - \beta_c|^{\nu'}$. By duality, the current-current correlation length of the XY model has the same behaviour. There has been a lot of debate in the literature about the value of ν' . Originally, it was believed that $\nu' = \nu/2$,⁷ but Kiometzis et al.⁴ later argued that the penetration depth does not get renormalized and would therefore have the mean-field exponent $\nu' = 1/2$. Finally, Herbut and Tesanovic⁸ found $\nu' = \nu$ using renormalization group arguments, and this value was later confirmed in Refs. 14,15,26 with different approaches. However, all these results rely on some analytical approximations. They also disagree with the results of superconductor experiments.^{9,10}

B. Broken/Coulomb phase

From the XY model point of view, the characteristic property of the broken phase ($\kappa > \kappa_c$) is non-zero magnetization $M \neq 0$. Another signal for symmetry breakdown is a non-zero value of the helicity modulus Υ . Through

XY: symmetric	$\kappa < \kappa_c$	critical	$\kappa = \kappa_c$	XY: broken	$\kappa > \kappa_c$
FZS: superconducting	$\beta > \beta_c$		$\beta = \beta_c$	FZS: Coulomb	$\beta < \beta_c$
$\xi = \mathcal{T}^{-1} \sim \kappa - \kappa_c ^{-\nu}$		$G_{\mathbf{x},\mathbf{y}} \sim \mathbf{x} - \mathbf{y} ^{-(1+\eta)}$		$\mathcal{T} = 0$	
$\lambda = m_\gamma^{-1} \sim \kappa - \kappa_c ^{-\nu'}$		$\Gamma_{ij}(\mathbf{p}) \sim \mathbf{p} ^{\eta_A}$		$\lambda = m_\gamma^{-1} = \infty$	
$\chi_A \sim \beta - \beta_c ^{-\gamma_A}$				$\Upsilon \sim \chi_m \sim \kappa - \kappa_c ^\nu$	

TABLE II: The behaviour of certain observables in the two phases of the models.

the duality, this corresponds to non-zero magnetic permeability χ_m in the Coulomb phase of the FZS.

In the extreme high-temperature limit $\beta \rightarrow 0$, the FZS approaches free non-compact electrodynamics, which is given by Eq. (1) in the limit $\kappa \rightarrow 0$. In this case, it is easy to calculate χ_m from the path integral, and we find

$$\chi_m \sim 1/\beta \quad \text{when } \beta \rightarrow 0. \quad (39)$$

Using Eqs. (26) and (29), we find $\Upsilon \rightarrow \kappa$ and $\chi \rightarrow 0$, as $\kappa \rightarrow \infty$.

As the critical point is approached χ_m vanishes, and following Ref. 25, we parameterize this with the critical exponent ν ,

$$\chi_m \sim |\beta - \beta_c|^\nu, \quad \beta \nearrow \beta_c. \quad (40)$$

By duality, the helicity modulus Υ must behave in the same way. It has been argued in Refs. 14,25,27 that $\nu = 1$.

C. Critical point

At the transition point, the spin-spin correlator in the XY model has a power-law decay $G_{\mathbf{x}_1, \mathbf{x}_2} \sim |\mathbf{x}_1 - \mathbf{x}_2|^{-(1+\eta)}$, where the anomalous dimension η has been measured to be $\eta \approx 0.038$.⁶

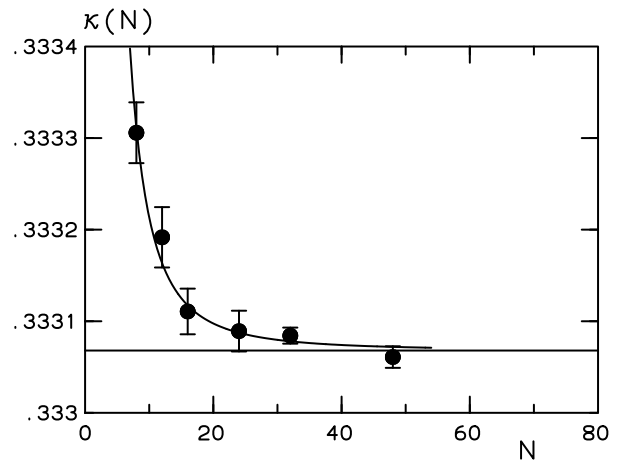
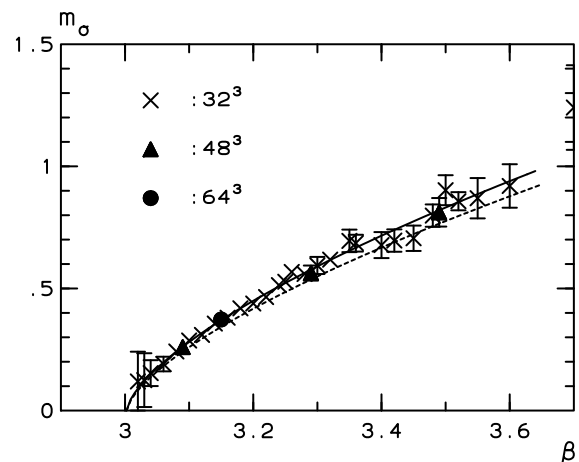
Similarly, one can define the anomalous dimension η_A for the photon correlator in the FZS by

$$\Gamma_{ij}(\mathbf{p}) \sim |\mathbf{p}|^{\eta_A}, \quad \text{when } |\mathbf{p}| \rightarrow 0. \quad (41)$$

Earlier studies have shown that $\eta_A \approx 1$.^{8,14,15,28}

V. LOCATING THE CRITICAL POINT

In order to explore the manifestations of the duality, we study both the FZS Eq. (5) and the XY model Eq. (7) using Monte Carlo simulations. For the FZS, the simulation algorithm consists of a single hit Metropolis update of the integer link variables, and for the XY model we use a Swendsen-Wang type reflection cluster algorithm.²⁹ One update sweep for the FZS consists of $N_1 N_2 N_3$ single link Metropolis hits, and for the XY model out of one full Swendsen-Wang cluster update. The number of Monte Carlo update sweeps typically ranges from 50000 to 10^7 , depending on lattice sizes and coupling constant values. The errors are determined by jackknife error calculation.

FIG. 1: Pseudocritical hopping parameter values $\kappa(N)$ as a function of the system size N in the XY model Eq. (7).FIG. 2: The scalar mass m in the XY model as a function of the dual coupling $\beta = 1/\kappa$. The solid curve shows the power-law fit in Eq. (44), and the dashed line the vortex tension fit in the FZS [see Eq. (58)].

Because of the duality, the critical points of the theories are related by $\beta_c = 1/\kappa_c$. We determined the critical coupling values

$$\kappa_c = 0.333068(7), \quad \beta_c = 3.00239(6) \quad (42)$$

by a numerical simulation of the XY model on cubic $N = N_1 = N_2 = N_3$ lattices with $N = 8-96$. For this,

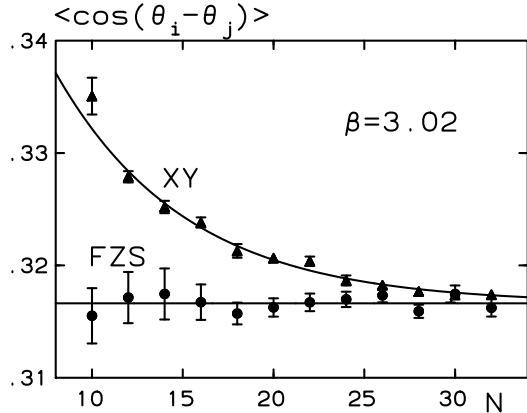


FIG. 3: A numerical check of duality relations for the nearest-neighbour correlator in Eq. (45) on a finite lattice.

we used the Binder cumulant method:³⁰ Matching the fourth-order cumulants of the magnetization measured from lattices of size N and $2N$ gives us an estimate of the N -dependent pseudocritical hopping parameter $\kappa_c(N)$. The results are shown in Fig. 1. Using the finite size scaling ansatz

$$\kappa_c(N) = \kappa_c + \frac{A_\kappa}{N^{1/\nu+\omega}}, \quad (43)$$

with $\omega \approx 0.8$ denoting the subleading XY model scaling exponent,⁶ we arrive at the numerical result in Eq. (42). The uncertainty in this value is small enough to have a negligible effect for the determination of the critical indices.

Most numerical studies of spin models with XY universality⁶ use the cosine action $s(x) = -\cos(x)$ rather than Eq. (4), and subsequently there is only limited experience with the Villain action. Nevertheless, there is no doubt that the phase transition with the Villain action is of second order and in the same universality class as with the cosine action. As an illustration we show the scalar mass $m = 1/\xi$ in the symmetric phase ($\kappa < \kappa_c$), as a function of the “temperature” $\beta = 1/\kappa$, in Fig. 2. The solid curve in the figure shows a χ^2 -fit with the scaling law

$$m(\beta) = A_\xi(\beta - \beta_c)^\nu \quad (44)$$

and with a fit with $\chi^2/\text{d.o.f.} = 0.35$ we obtain the parameter values $A_\xi = 1.32(4)$ and $\nu = 0.66(2)$, in agreement with the cosine action results.⁶ The amplitude value A_ξ is important for the comparison with the vortex tension in the gauge theory, to be discussed below.

VI. VORTEX TENSION

In order to illustrate the numerical consequences of the duality we measured the nearest-neighbour spin-spin

correlation function,

$$G_{\mathbf{x}+i,\mathbf{x}} = \langle \cos(\theta_{\mathbf{x}+i} - \theta_{\mathbf{x}}) \rangle_{XY} \quad (45)$$

in the XY model at $\beta = 1/\kappa = 3.02$. In the gauge theory, this is mapped to the expectation value of

$$\langle e^{\beta P_{\mathbf{x},ij} - \beta/2} \rangle_{\text{FZS}}. \quad (46)$$

In Fig. 3 we compare both measurements as functions of the system size N on cubic boxes with periodic boundary conditions. It is evident that Eq. (12), and thereby the duality, only is valid for infinite systems, i.e., the boundary conditions of finite systems do not respect our duality arguments. The curves in the figure assume finite volume corrections of the form $\exp(-cN)$ and extrapolate to the same value in the thermodynamic limit.

Let us now consider the long-distance behaviour of the correlation function $G_{\mathbf{x}_1,\mathbf{x}_2}$ defined in Eq. (17). The duality maps this correlator into Eq. (20) in the FZS. In principle, we could measure Eq. (20) directly, but it turns out to be more convenient to use an indirect approach, which was introduced in Ref. 20.

As we shall now show, Eq. (20) corresponds exactly to a vortex, or an Abrikosov flux tube, in the FZS. Thus, the spin-spin correlation length ξ in the XY model is exactly the tension \mathcal{T} , the vortex free energy per unit length, in the FZS. These flux tubes exist because a superconductor resists applied external magnetic fields. For field strengths above the critical field H_{c1} magnetic flux penetrates the material, and the flux arranges into vortex lines, Abrikosov flux tubes.

In practice, we define the vortex tension as follows: Using appropriate modifications of periodic boundary conditions, to be described below, we constrain the net number of vortex lines n_V winding around the finite volume to, say, z direction. The vortex tension \mathcal{T} is then defined by

$$\mathcal{T} = -\frac{1}{N_3} \ln \left[\frac{Z_{\text{FZS}}(n_V = 1)}{Z_{\text{FZS}}(n_V = 0)} \right], \quad (47)$$

in the $N_3 \rightarrow \infty$ limit.

Let us now discuss how the appropriate boundary conditions are constructed. Labelling the cartesian coordinates $\mathbf{x} = (n_1, n_2, n_3)$, $n_i = 1, \dots, N_i$ $i = 1, \dots, 3$, and using periodic boundary conditions to all directions

$$\begin{aligned} I_{(n_1=N_1+1, n_2, n_3), i} &= I_{(n_1=1, n_2, n_3), i}, \\ I_{(n_1, n_2=N_2+1, n_3), i} &= I_{(n_1, n_2=1, n_3), i}, \\ I_{(n_1, n_2, n_3=N_3+1), i} &= I_{(n_1, n_2, n_3=1), i}, \end{aligned} \quad (48)$$

the total magnetic flux $\Phi = 2\pi n_V$ through any planar 2-dimensional cross section $\Omega_{i,j}$ of the lattice

$$\Phi(\Omega_{i,j}) = 2\pi \sum_{p \in \Omega_{i,j}} I_p(i, j), \quad i \neq j \quad (49)$$

equals zero because of the periodicity. However, if we choose a set of links $I_{(n_1, n_2, n_3), 2}$, with $n_1 = 1, n_2 = 1$ and $n_3 = 1 \dots N_3$, and use a “twisted” boundary condition

$$I_{(N_1+1, 1, n_3), 2} = I_{(1, 1, n_3), 2} + n_V, \quad n_3 = 1, \dots, N_3, \quad (50)$$

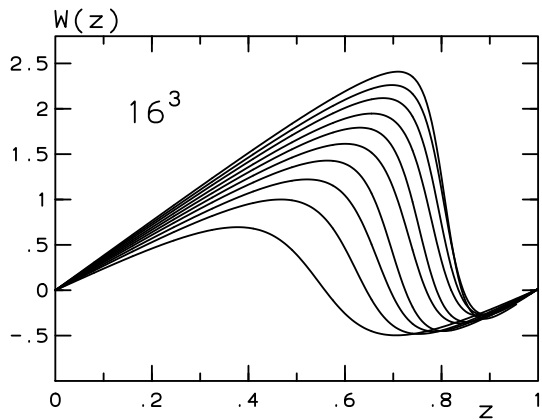


FIG. 4: The function $W(z)$ measured from 16^3 -lattice, with β varying from 3.0 (bottom curve) to 4.0 (top).

the flux through N_3 cross sectional areas $\Omega_{1,2}$ acquires the value $\Phi(\Omega_{1,2}) = 2\pi n_V$. At $n_V = 1$ this corresponds to a single vortex of length $L = N_3$. The vortex line forms a closed loop through the z -direction of the box.

It should be noted that the modification of the boundary condition does not give the modified link a special status: by a suitable redefinition of the link variables I_j , the “twist” can be moved to arbitrary location along the $(1,2)$ -plane, also away from the boundary.

In practice, a more convenient way to implement the fixed flux is to consider a system with fully periodic boundary conditions but with a modified action: Let us define a plaquette field which is non-zero only on one fixed “stack” of $(1,2)$ -plaquettes,

$$m_{\mathbf{x},i} = \begin{cases} 1 & \text{if } x_1 = x_2 = 1; i = 3, \\ 0 & \text{otherwise} \end{cases}. \quad (51)$$

Now we can define the partition function

$$Z_{\text{FZS}}(\beta, n_V) =$$

$$\begin{aligned} W(z) &\equiv \frac{\partial \log Z_{\text{FZS}}(\beta, z)}{\partial z} \\ &= \frac{1}{Z_{\text{FZS}}(\beta, z)} \frac{\beta}{N_3} \sum_{\{I_{\mathbf{x},i}\}} \left[\sum_{\mathbf{x},i} \left(\frac{1}{2} \epsilon_{ijk} P_{\mathbf{x},jk} - z m_{\mathbf{x},i} \right) m_{\mathbf{x},i} \right] \exp \left(-\frac{\beta}{2} \sum_{\mathbf{x},i} \left(\frac{1}{2} \epsilon_{ijk} P_{\mathbf{x},jk} - z m_{\mathbf{x},i} \right)^2 \right), \end{aligned} \quad (55)$$

which can be determined with Multicanonical Monte Carlo simulations (for technical details, we refer to Ref. 20). In Fig. 4, we show the function $W(z)$ measured from a 16^3 volume as a function of z for several values for β . β -values in the superconducting phase and close to the

$$\sum_{\{I_{\mathbf{x},i}\}} \exp \left[-\frac{\beta}{2} \sum_{\mathbf{x},i} \left(\frac{1}{2} \epsilon_{ijk} P_{\mathbf{x},jk} - n_V m_{\mathbf{x},i} \right)^2 \right] \quad (52)$$

which is equivalent to the partition function with the unmodified action but with the boundary condition Eq. (50). (Again, the choice $x_1 = x_2 = 1$ here is arbitrary.)

Comparison of Eq. (52) with Eq. (20) shows that the vortex tension in Eq. (47) is closely related to the XY model spin correlator $G_{\mathbf{x}_1, \mathbf{x}_2}$, provided that we identify $m_{\mathbf{x},i}$ with $\alpha_{\mathbf{x},i}$. Indeed, the only difference is that $m_{\mathbf{x},i}$ does not have start or end points, but stretches across the whole system. However, on a periodic lattice, we can imagine moving the source \mathbf{x}_1 of $\alpha_{\mathbf{x},i}$ through the boundary to \mathbf{x}_2 so that it cancels the sink. This leads to a sourceless field which has one field line passing through the lattice, and this shows that in the infinite volume limit the XY model correlation length ξ and the vortex tension \mathcal{T} are related by

$$\mathcal{T} = 1/\xi = m. \quad (53)$$

As an aside, we note that this procedure does not make sense for the XY model spin correlators, since now $G_{\mathbf{x}, \mathbf{x} + \hat{e}_3 N_3} = G_{\mathbf{x}, \mathbf{x}} = 1$, again showing that the periodic boundary conditions in a finite volume do not respect the duality relation.

In practice, all measurements are affected by the finite size of the lattices and by the performance of the numerical algorithms, and it is therefore interesting to compare the direct measurement of \mathcal{T} with the measurement of m in the XY model. In order to measure \mathcal{T} in simulations, we write it as an integral

$$\mathcal{T} = \int_0^1 W(z) dz \quad (54)$$

over an expectation value $W(z)$

critical point.

The vortex tension \mathcal{T} vanishes in the Coulomb phase and at criticality $\beta = \beta_c$. In Fig. 5 we show the measured value of \mathcal{T} as a function of the lattice size N , using $\beta = 3.0016$, which is very close to β_c in the Coulomb phase. The tension decreases with increasing linear size

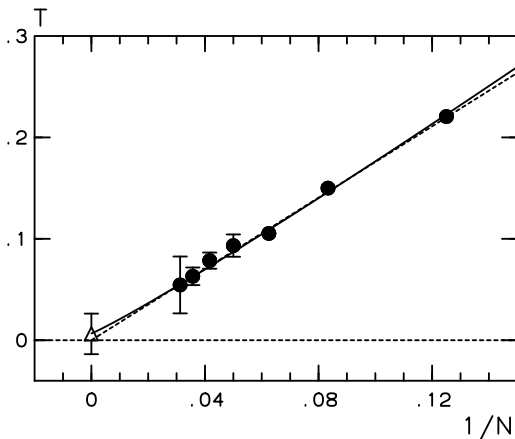


FIG. 5: The tension \mathcal{T} at $\beta = 3.0016$ (slightly below β_c , i.e. in the Coulomb phase) as a function of N^{-1} . In the infinite-volume limit, the tension extrapolates to zero.

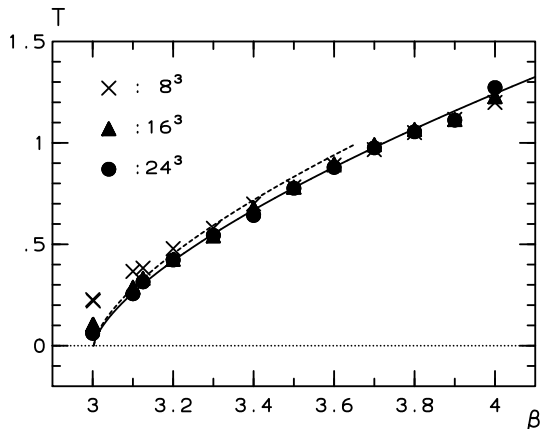


FIG. 6: The tension \mathcal{T} on 8^3 , 16^3 and 24^3 lattices and a fit to 24^3 data in the superconducting phase of the FZS. The solid line corresponds to the fit in Eq. (58) and the dashed line to the XY model mass in Eq. (44).

N , and assuming finite size corrections of the form $N^{-\alpha}$ we obtain the fit

$$\mathcal{T}(N) = 0.006(26) + 2.0(7) N^{-\alpha}, \quad \alpha = 1.1(2), \quad (56)$$

with $\chi^2/\text{d.o.f.} = 0.50$ for the fit. The data support a vanishing tension in the Coulomb phase close to criticality. The value of α is consistent with $\alpha = 1$ and, at criticality and in the dual XY model $\alpha = 1$ corresponds to a scalar correlation length finite size scaling $\xi(N) \propto N$. Fixing $\alpha = 1$ we obtain the fit

$$\mathcal{T}(N) = \frac{1.76(3)}{N} \quad \beta \approx \beta_c \quad (57)$$

at the $\chi^2/\text{d.o.f.}$ value of 0.65 for the fit.

In the superconducting phase, we calculated the vortex tension \mathcal{T} using 8^3 , 16^3 and 24^3 lattices; the results are presented in Fig. 6 as functions of β . The finite size

effects between 16^3 and 24^3 lattices are smaller than the statistical errors. We fit the 24^3 data in a broad scaling interval $3.05 < \beta < 4.1$ with the power-law behaviour

$$\mathcal{T}(\beta) = A_{\mathcal{T}}(\beta - \beta_c)^{\nu_{\mathcal{T}}}, \quad (58)$$

where $\nu_{\mathcal{T}}$ denotes the tension scaling exponent. We obtain the parameter values $A_{\mathcal{T}} = 1.24(2)$ and $\nu_{\mathcal{T}} = 0.672(9)$ with a $\chi^2/\text{d.o.f.}$ value of 1.13 for the fit.

The duality (53) implies that $A_{\mathcal{T}}$ and $\nu_{\mathcal{T}}$ ought to be equal to the XY model quantities A_{ξ} and ν in Eq. (44). Indeed, we find that $\nu_{\mathcal{T}}$ agrees with the XY model exponent $\nu = 0.671$, and that $A_{\mathcal{T}}/A_{\xi} \approx 0.94(5)$. In summary, the vortex tension $\mathcal{T}(\beta)$ of the gauge theory agrees within two standard deviations of the gauge theory errors with the scalar mass $m(\kappa = 1/\beta)$ of the XY model. This constitutes a highly non-trivial test for the methods developed in Ref. 20.

VII. SUSCEPTIBILITIES

We shall now discuss the susceptibilities χ_m and χ_A defined in Eqs. (36) and (37), respectively. We also generalize the definition of χ_A to non-zero momenta by

$$\chi_A(\mathbf{p}) = \frac{\Gamma_{33}(\mathbf{p})}{p_{\Lambda(1,2)}^2}, \quad (59)$$

where $p_{\Lambda(1,2)}^2$ is defined as

$$p_{\Lambda(1,2)}^2 = 2 \sum_{i=1}^2 [1 - \cos p_i] = 2 \sum_{i=1}^2 [1 - \cos(2\pi k_i/N_i)]. \quad (60)$$

We use the lowest momentum value for the (1,2)-plane momentum, but non-zero values of the z -component of the momentum $p_3 = 2\pi k_3/N_3$. We expect the momentum dependence of the susceptibility to be a function of the total lattice momentum squared

$$p_{\Lambda}^2 = 2 \sum_{i=1}^3 [1 - \cos p_i] = 2 \sum_{i=1}^3 [1 - \cos(2\pi k_i/N_i)]. \quad (61)$$

As discussed in Sections IV A and IV B, at zero momentum χ_A is finite and non-zero in the superconducting phase and diverges in the Coulomb phase, whereas χ_m vanishes in the superconducting phase and is non-zero in the Coulomb phase, being equal to the helicity modulus Υ of the XY theory.

Our measurements demonstrate the presence of a massless photon pole in the Coulomb phase of the gauge theory. At $\beta = 2.0$ – well within the Coulomb phase – we determine the susceptibility $\chi_A(\mathbf{p})$ on 16^3 , 32^3 , 48^3 and 64^3 lattices as a function of small momentum values \mathbf{p} . The results are shown in Fig. 7 as a function of $\ln p_{\Lambda}^{-2}$. The data are fitted with the form

$$\chi_A(\mathbf{p}) = \frac{0.46(1)}{p_{\Lambda}^2} \quad \beta = 2.0, \quad (62)$$

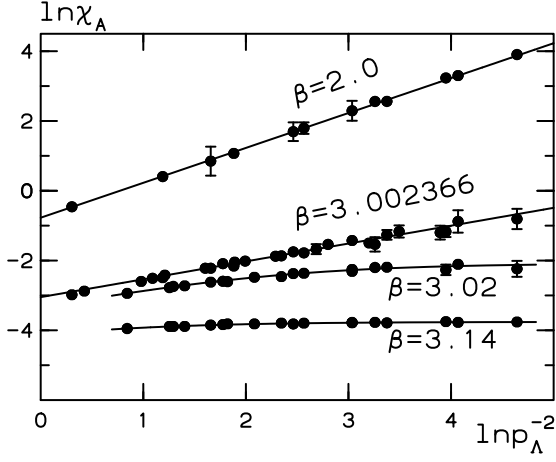


FIG. 7: Logarithm of the gauge field susceptibility $\ln \chi_A(\mathbf{p})$ as a function of $\ln p_\Lambda^{-2}$ in the Coulomb phase at $\beta = 2.0$ (top curve), at the critical point $\beta = \beta_c$ (second curve from above), and for two β -values in the superconducting phase.

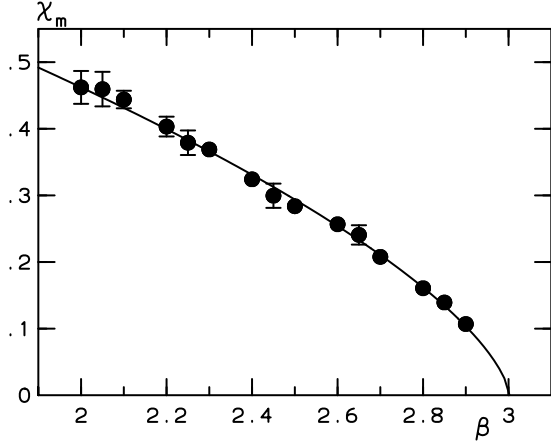


FIG. 8: The magnetic permeability χ_m as a function of β in the Coulomb phase. The curve corresponds to the fit in Eq. (63).

with $\chi_{d.o.f.}^2 = 0.67$ for the fit. This is equivalent to saying that in the zero-momentum limit, $\chi_m = 0.46(1)$ at $\beta = 2.0$. This value is slightly smaller than the result from free electrodynamics in Eq. (39).

In fact, since $\chi_A(\mathbf{p})$ is essentially the gauge field correlation function, albeit in a gauge-invariant form, the divergence $1/p_\Lambda^2$ demonstrates the presence of a massless photon. Thus, we can interpret $\chi_m = \Upsilon$ as the corresponding wave function renormalization Z factor.

As the critical point is approached from the Coulomb phase χ_m vanishes with the exponent ν , as discussed in Section IV B. The measured values of χ_m are presented in Fig. 8, together with the fit to the scaling ansatz

$$\chi_m(\beta) = A_\Upsilon(\beta_c - \beta)^\nu. \quad (63)$$

The parameter values are $A_\Upsilon = 0.46(1)$ and $\nu = 0.66(2)$

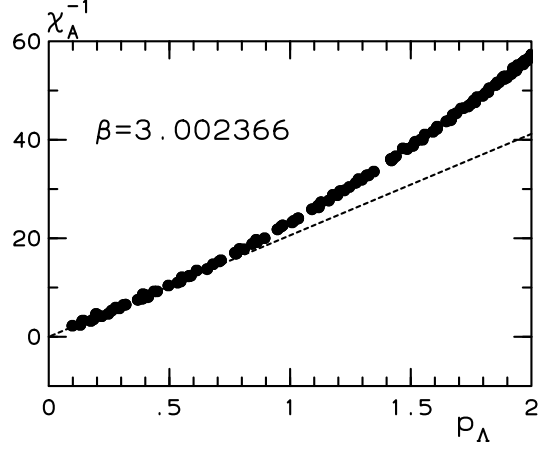


FIG. 9: The inverse gauge susceptibility $\chi_A^{-1}(\mathbf{p})$ at the critical point $\beta = 3.002366$ for $16^3, 24^3, 32^2 \times 64, 36^3, 44^3, 48^3$ and 64^3 lattices as a function of p_Λ . The dashed line corresponds to Eq. (67).

and the fit has a $\chi_{d.o.f.}^2$ value of 0.32. By duality, this is exactly the scaling of Υ near the critical point in the XY model, and the value of ν is indeed entirely consistent with arguments that Υ scales with the exponent ν .²⁵ The amplitude value A_Υ could also be compared directly with the XY model, but we are not aware of helicity modulus data for the Villain action.

The anomalous dimension η_A of the gauge field at criticality can be obtained from the momentum dependence of the gauge field susceptibility $\chi_A(\mathbf{p})$ as

$$\chi_A(\mathbf{p}) = c_A(p_\Lambda^2)^{\eta_A/2-1} \quad \beta = \beta_c, \quad (64)$$

for low \mathbf{p} . We show the data together with a power law fit in Fig. 7, as well as in Fig. 9. The fit to Eq. (64) gives the exponent

$$\eta_A = 0.98(4), \quad (65)$$

which is perfectly consistent with the value $\eta_A = 1$ predicted in Refs. 8,28. If we fix $\eta_A = 1$, we obtain the critical amplitude

$$c_A = 20.7(3), \quad (66)$$

which implies

$$\chi_A(\mathbf{p}) = \frac{0.0484(7)}{p_\Lambda}, \quad (67)$$

for small momenta. This fit is shown as a straight dashed line in Fig. 9.

In the superconducting phase of the FZS the magnetic permeability χ_m vanishes at zero momentum, and therefore the photon becomes massive. The gauge field susceptibility $\chi_A(\mathbf{p})$ tends to a finite limit as $\mathbf{p} \rightarrow 0$. This

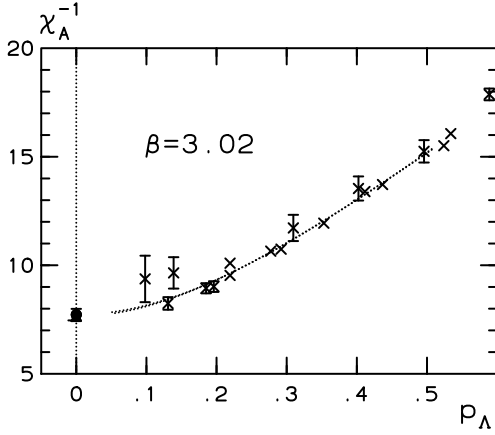


FIG. 10: $\chi_A^{-1}(\mathbf{p})$ at $\beta = 3.02$ in the superconducting phase for $32^2 \times 64$, 48^3 and 64^3 lattices as a function of p_Λ . The two dotted lines, which are barely distinguishable, correspond to fits using Eqs. (69) and (72) and extrapolate to finite values at zero momentum.

is shown in Fig. 7, where the lowest two data sets of the figure correspond to χ_A in the superconducting phase.

At the critical point ($\beta = \beta_c$), $\chi_A(\mathbf{p})$ is proportional to $p^{\eta_A - 2}$ [see Eq. (64)]. The phase transition in the FZS is continuous, and therefore the analytic form of $\chi_A(\mathbf{p})$ at non-zero momenta must interpolate smoothly between the critical, massless behaviour and the massive mode in the superconducting phase. This reasoning leads to the Fisher scaling relation

$$\nu' = \frac{\gamma_A}{2 - \eta_A}. \quad (68)$$

Perhaps the simplest way in which this could happen is if the susceptibility has the form

$$\chi_A^{-1}(\mathbf{p}) = c_A (p_\Lambda^2 + m_\gamma^2)^{1 - \eta_A/2}, \quad (69)$$

which would correspond to the asymptotic behaviour

$$\Gamma(\tau, \mathbf{p} = 0) \sim \tau^{-\eta_A/2} \exp(-m_\gamma \tau), \quad (70)$$

of the photon correlation function.

In the $\mathbf{p} = 0$ limit Eq. (69) relates the photon mass and the gauge field susceptibility χ_A through

$$\chi_A = \frac{1}{c_A m_\gamma^{2 - \eta_A}}. \quad (71)$$

While the precise form of the ansatz does not affect the scaling relation (68), it would lead to a systematic error in the determination of m_γ . To estimate these errors, we also consider an ansatz based on treating the dual XY model as a theory of a free complex scalar field (see Appendix A),

$$\chi_A(\mathbf{p}) = \frac{4 c_A}{\pi p^2} \left[\frac{m_\gamma}{2} + \frac{p^2 - m_\gamma^2}{2p} \arctan \frac{p}{m_\gamma} \right]. \quad (72)$$

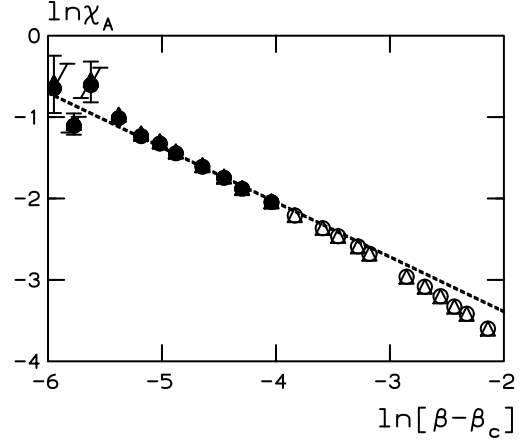


FIG. 11: $\ln \chi_A$ as a function of $\ln(\beta - \beta_c)$ in the superconducting phase, together with power law fits.

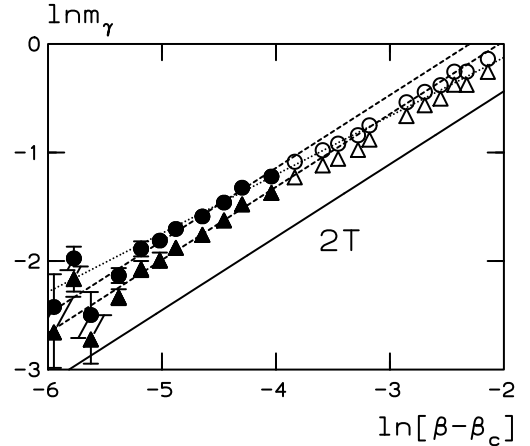


FIG. 12: The logarithm of the photon (pole) mass m_γ , together with power-law fits (dashed lines) and the theoretical expectation $m_\gamma = 2T$. The circles and triangles correspond to zero-momentum extrapolations using ansätze (69) and (72), respectively. The dashed lines show fits to the filled symbols with the XY model exponent $\nu' = \nu_{XY}$. The dotted line is the same as the solid line in Fig. 17.

Again, m_γ gives the exponential decay rate of the correlator, and at the critical point the ansatz agrees with Eq. (64). However, Eq. (71) becomes

$$\chi_A = \frac{8}{3\pi} \frac{1}{c_A m_\gamma}. \quad (73)$$

Therefore, we can estimate that the systematic error in the determination of m_γ is roughly $3\pi/8 - 1 \approx 20\%$.

As an example, we show χ_A^{-1} at $\beta = 3.02$ in Fig. 10, together with fits of momenta $0 < p_\Lambda < 0.5$ to Eqs. (69) and (72). There is practically no difference between the fits, but the fit parameters c_A and m_γ are different.

Performing the fit to Eqs. (69) and (72) at several $\beta > \beta_c$ we obtain $\chi_A \equiv \chi_A(\mathbf{p} \rightarrow 0)$ and m_γ as functions of β .

The results for $\chi_A(\beta)$ and $m_\gamma(\beta)$ are shown in Figs. 11 and 12.

The gauge field susceptibility $\chi_A(\beta)$ clearly has a power law divergence as we approach the critical point. Fitting the ansatz $\chi_A = A_\chi(\beta - \beta_c)^{-\gamma_A}$ to the datapoints shown by full symbols in Fig. 11, we obtain

$$\begin{aligned} \gamma_A &= 0.68(3) \quad \text{for Eq. (69),} \\ \gamma_A &= 0.70(4) \quad \text{for Eq. (72),} \end{aligned} \quad (74)$$

both of which are compatible with the result $\gamma_A = \nu_{XY}$ obtained in Ref. 14. Assuming $\gamma_A = \nu_{XY}$, we obtain

$$\begin{aligned} A_\chi &= 0.00871(15) \quad \text{for Eq. (69),} \\ A_\chi &= 0.00888(17) \quad \text{for Eq. (72).} \end{aligned} \quad (75)$$

The critical behaviour of the photon mass $m_\gamma(\beta)$ (or equivalently, the penetration depth) is more subtle. Inserting the measured values for η_A and γ_A in Eq. (68), we obtain the critical exponent

$$\begin{aligned} \nu' &= 0.67(4) \quad \text{for Eq. (69),} \\ \nu' &= 0.69(5) \quad \text{for Eq. (72).} \end{aligned} \quad (76)$$

This result is fully compatible with the prediction $\nu' = \nu_{XY}$.^{8,14,15,26}

Similarly, the scaling ansätze fix the critical scaling function $m_\gamma = A_\gamma(\beta - \beta_c)^{\nu'}$ through Eqs. (71) and (73),

$$\begin{aligned} A_\gamma &= \frac{1}{c_A(\beta_c)A_\chi} = 4.69(8), \quad \text{for Eq. (69),} \\ A_\gamma &= \frac{8}{3\pi} \frac{1}{c_A(\beta_c)A_\chi} = 3.94(6), \quad \text{for Eq. (72).} \end{aligned} \quad (77)$$

The corresponding critical scaling functions for m_γ are shown in Fig. 12 as dashed lines. The scaling functions only agree with direct mass measurements in a narrow region near the critical point. In fact, the direct mass measurements would favour slightly critical exponents for the photon mass

$$\begin{aligned} \nu' &= 0.58(3), \quad \text{for Eq. (69),} \\ \nu' &= 0.62(3), \quad \text{for Eq. (72).} \end{aligned} \quad (78)$$

The reason for this discrepancy is that c_A changes rather rapidly as a function of β when the critical point is approached. This is shown in Fig. (13). Using the critical value of c_A in Eqs. (71) and (73) is therefore justified only very close to the critical point.

Since the photon mass and the vortex tension scale with the same exponent, it makes sense to calculate the the amplitude ratio A_γ/A_T . We find

$$\begin{aligned} A_\gamma/A_T &= 3.8, \quad \text{for Eq. (69),} \\ A_\gamma/A_T &= 3.2, \quad \text{for Eq. (72).} \end{aligned} \quad (79)$$

These values are significantly greater than the expected value of 2, which follows from the assumption that if $m_\gamma > 2T$, the photon should be able to decay into two

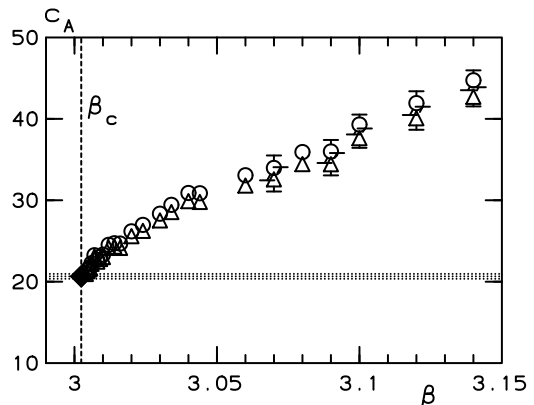


FIG. 13: The value of c_A determined from fits to Eq. (69) [circles] and Eq. (72) [triangles].

vortices,¹ and this would result in exponential decay with rate $2T$. We see two plausible reasons for this behaviour: Firstly, it is likely that our ansätze (69) and (72) are not of the right form. In this case, it would be important to find a theoretically better motivated ansatz, which could then be tested numerically by fitting it to our measurements. The correct functional form should yield $A_\gamma/A_T = 2$. Secondly, the volumes available for our analysis may be too small. Vortex-vortex interactions are presumably not negligible if the lattice size is of order $1/m_\gamma$, which modifies the “free vortex” behaviour $m_\gamma = 2T$.

On the other hand, it may also be possible that the system has a massive photon state, similar to resonances in particle physics, which would eventually decay into two vortices at distance longer than what we can probe in our simulations.

VIII. PHOTON MASS

In this section, we shall discuss the determination of the penetration depth λ , or equivalently the photon mass $m_\gamma = 1/\lambda$, directly from the decay of the correlator $\Gamma(\tau, \mathbf{p})$ in Eq. (33). This approach is less likely to be sensitive to systematic errors than the pole mass determination.

We note that the current operator $\Delta_{\mathbf{x},i}^{XY}$, i.e., the dual of the photon, has odd parity with respect to reflections of the gradient angle $\theta_{\mathbf{x}+i} - \theta_{\mathbf{x}}$. The more standard compact functions of the gradient angle

$$O_o(\mathbf{x}, i) = i\beta^{-1} \sin(\theta_{\mathbf{x}+i} - \theta_{\mathbf{x}}) \quad (80)$$

$$O_e(\mathbf{x}, i) = \beta^{-1} \cos(\theta_{\mathbf{x}+i} - \theta_{\mathbf{x}}) \quad (81)$$

have odd and even parity respectively. The correlation functions of these observables map to correlation func-

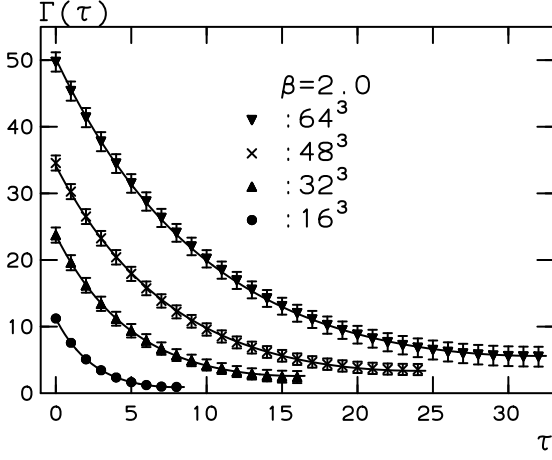


FIG. 14: Correlation function $\Gamma(\tau)$ at $\beta = 2.0$ in the Coulomb phase. The fitted curves correspond to the massless photon.

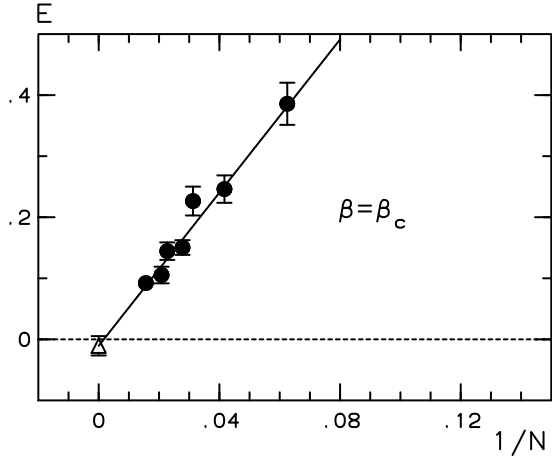


FIG. 15: Photon energy at $\beta = \beta_c$. The straight line extrapolates to vanishing photon mass at criticality.

tions of

$$O_o(\mathbf{x}, ij) = e^{-\frac{\beta}{2}} \sinh(\beta P_{\mathbf{x},ij}) \quad (82)$$

$$O_e(\mathbf{x}, ij) = e^{-\frac{\beta}{2}} \cosh(\beta P_{\mathbf{x},ij}) \quad (83)$$

in the FZS, again with definite parity.

We measure the photon mass from symmetric N^3 and elongated $N_3 > N_2 = N_1$ periodic lattices, using the lowest non-zero value of the momentum

$$\underline{\mathbf{p}} = \left(\frac{2\pi}{N_1}, 0 \right). \quad (84)$$

The asymptotic decay of the photon correlation function $\Gamma(\tau, \underline{\mathbf{p}}) \sim e^{-E(\underline{\mathbf{p}})\tau}$ is governed by the lattice dispersion relation

$$E(\underline{\mathbf{p}}) = \sqrt{p_{\Lambda(1,2)}^2 + \hat{m}_\gamma^2 + \Sigma(\underline{\mathbf{p}})}, \quad (85)$$

where

$$\hat{m}_\gamma = \frac{1}{2} \sinh\left(\frac{m_\gamma}{2}\right). \quad (86)$$

The photon self energy $\Sigma(\underline{\mathbf{p}})$ is expected to be small for large lattice sizes, and for the data used in this work it is unobservable.

The photon is massless in the Coulomb phase of the gauge theory. In Fig. 14 we show the correlation functions $\Gamma(\tau)$ at $\beta = 2$ measured from $16^3 - 64^3$ lattices. The curves in the figure are fits to the data, assuming vanishing photon mass and no anomalous dimension,

$$\Gamma(\tau) = A \left[e^{-\tau \sqrt{2[1-\cos(2\pi/N_1)]}} + e^{-(N_3-\tau) \sqrt{2[1-\cos(2\pi/N_1)]}} \right] + \text{const} \quad (87)$$

which yields a perfect fit to the data.

The photon mass also vanishes at the critical point $\beta = \beta_c$, but there one must take into account the non-zero anomalous dimension $\eta_A = 1$. Instead of a pure exponential fit, we assume the asymptotic behaviour in Eq. (70) and use the ansatz

$$\Gamma(\tau) = A[\tau^{-1/2} e^{-\tau E} + (N_3 - \tau)^{-1/2} e^{-(N_3-\tau)E}] + \text{const} \quad (88)$$

in our fits.

On Fig. 15 we show the energy of the photon state with $|\underline{\mathbf{p}}| = 2\pi/N$, measured from cubical N^3 lattices, as a function of $1/N$. Fitting the data with the form

$$E(N) = E(N = \infty) + A_E N^{-1}, \quad \beta = \beta_c, \quad (89)$$

we obtain a vanishing photon energy $E(N = \infty) = 0.01(2)$ and $A_E = 6.3(6)$ with $\chi^2/\text{d.o.f.}$ value of 1.20 for the fit. The value of A_E agrees very well with the value 2π expected if $E(\underline{\mathbf{p}}) = (p_{\Lambda(1,2)}^2)^{1/2}$.

Let us now turn to the photon mass in the superconducting phase. At fixed $\beta = 3.01$ we compare the finite-momentum photon correlation functions and correlation functions of the observables O_e and O_o in the FZS with their dual counterparts in the XY model. The simulations are carried out on 64×32^2 lattices with high statistics of about 10^6 sweeps. Fig. 16 displays three $|\underline{\mathbf{p}}| = 2\pi/32$ correlation functions for (a) the FZS and (b) the XY model. The corresponding correlation functions of the FZS are not identical to the ones in the XY model, as the duality is only exact for infinite systems.

Again we use the ansatz in Eq. (88) to fit the data. The fits are done in the τ interval $4 \leq \tau \leq 32$. For the photon mass, we obtain the values $m_\gamma = 0.08(3)$ in the FZS and $m_\Delta = 0.06(3)$ for its dual in the XY model. The values are consistent with each other and also with twice the XY scalar mass value $m(\beta = 3.01) \approx 0.05(1)$, but the statistical errors are large.

Mass values from the odd parity O_o correlation functions have the values 0.10(4) in the FZS and 0.06(3) in the XY model and therefore are degenerate with the photon mass. For the even parity O_e operator, we obtain the mass 0.28(2) in the FZS and 0.25(1) in the XY model.

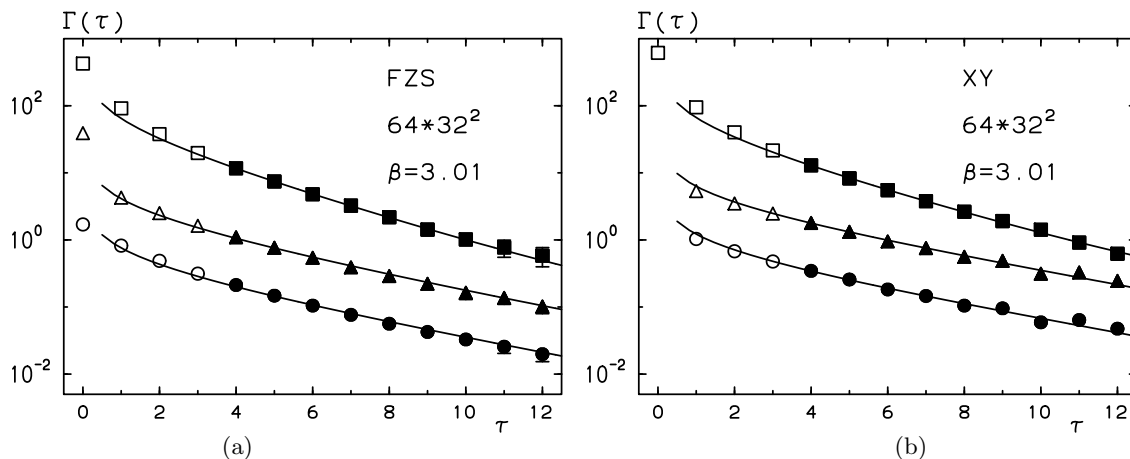


FIG. 16: (a) Correlation functions in the FZS and (b) their dual map in the XY model. The data is at $\beta = 3.01$, in the superconducting phase of the FZS. From bottom to top, the curves are the photon, O_o and O_e in the FZS and their duals in the XY model.

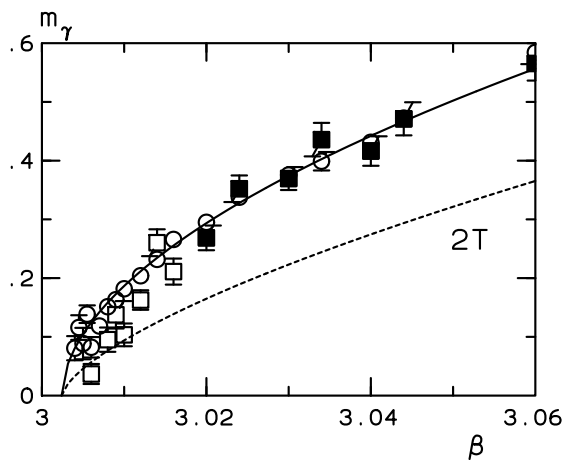


FIG. 17: The photon mass m_γ in the superconducting phase as a function of β . The squares show the values determined from the exponential decay of the photon correlation function, and the circles show the pole mass values from fits to Eq. (69) in Sect. VII. The solid line is a power law fit to measured values of m_γ . (Only filled squares are used in the fit). The dashed line shows the decay rate $m_\gamma = 2T$, which corresponds to an unstable photon decaying into two vortices.

In order to obtain the critical behaviour of the photon mass m_γ in the superconducting phase, we repeat the correlation function analysis at several values of $\beta > \beta_c$, using lattices of sizes 48^3 and 64×32^2 . The final results are shown as circles in Fig. 17. For comparison, the figure also shows m_γ determined from the finite momentum dispersion of the gauge field susceptibility $\chi_A(\mathbf{p})$ in Section VII. Neglecting the points very close to β_c and assuming a power law singular scaling behavior

$$m_\gamma(\beta) = A_\gamma(\beta - \beta_c)^{\nu'}, \quad (90)$$

a fit in the range $3.02 \leq \beta \leq 3.06$ to m_γ from the correlation functions (squares) yields $A_\gamma = 2.6(5)$ and $\nu' = 0.54(6)$ with $\chi^2/\text{d.o.f.} = 1.3$ for the fit. This value for the exponent $\nu' \approx 1/2$ is inconsistent with the XY value $\nu_{XY} \approx 2/3$. It agrees with the mean field value, as was predicted in Ref. 4 and observed experimentally in Ref. 10.

However, as we already argued in Section VII, the scaling law Eq. (90) with $\nu' \approx 0.5$ describes only pre-asymptotic scaling, and the true critical exponent $\nu' = \nu_{XY}$. As the measured values of m_γ are higher than $2T$, we expect the photon to decay into two vortices, which would lead to $\nu' = \nu_{XY}$, but also to $m_\gamma = 2T$. This behaviour is shown in Fig. 17 by the dashed line, and is clearly incompatible with the direct mass measurements except in very close proximity of the critical point. However, the statistical uncertainty of the data in this region is too large to justify quantitative comparison. A possible source for the overall discrepancy is the fact that both the lattice sizes and the distance where the mass is extracted from the correlation functions is of order $1/m_\gamma$, while in order to be able to neglect vortex interactions and observe $m_\gamma \sim 2T$, distances and lattice sizes much larger than this are required. This is very difficult to achieve in practice.

We also remark a further complication in the photon mass measurements. Our simulations, which typically run for about 10^6 Monte Carlo sweeps, exhibit from time to time “exceptional configurations” with large contributions to the photon correlator at large τ -distances. We suspect that excitations of the vortex loop network are responsible. Indeed, it is easy to see that a vortex-antivortex pair wrapping around the finite lattice to the z direction also contributes to the photon correlation function in Eq. (33). These configurations can significantly affect the measurements, unless the lattice size is again much larger than the inverse vortex tension.

IX. CONCLUSIONS

In this paper, we have used numerical techniques to explore the duality between the three-dimensional integer gauge theory and the XY model in the Villain formulation. Our aim was to identify the ways in which the duality manifests itself in the correspondence between observables and the critical exponents of the two models.

First, we used the duality to test the method developed in Ref. 20 for measuring the vortex tension. The results agree perfectly with the direct measurements of the correlation length in the XY model. Similar methods can be used in (and were originally developed for) more complicated theories, which do not have an exact dual description.

Second, we investigated the critical behaviour of the magnetic field of the gauge theory, which is dual to the Noether current of the XY model. We measured the anomalous dimension η_A at the critical point, as well as the scaling exponents γ_A and ν of the gauge field susceptibility and the magnetic permeability. Our results are compatible with predictions $\eta_A = 1$,²⁸ $\gamma_A = \nu_{XY} \approx 0.6723$,¹⁴ and $\nu = \nu_{XY}$.^{14,25,27}

These results, together with the Fisher scaling relation (68), imply that the photon mass (or the penetration depth λ) scaling exponent ν' must be equal to the XY model critical exponent: $\nu' = \nu_{XY}$.⁸ Our results support this prediction, but only in extremely close proximity to the critical point.

The non-trivial anomalous dimension makes the determination of the photon mass extremely difficult and prone to systematic errors. The ratio of the photon mass to the vortex tension was $A_\gamma/A_{\mathcal{T}} \approx 3 - 4$ in the various approaches we tried. This means that the photon ought to decay into two vortices and the photon correlator should decay with rate $2\mathcal{T}$ at long distances. Our

data seems compatible with this very close to the critical point, but is not conclusive because of large statistical and systematical uncertainties.

Nonetheless, we believe that the photon does indeed decay and the high ratio $A_\gamma/A_{\mathcal{T}}$ is due to an incorrect ansatz for the propagator. Were the true form of the propagator in the proximity of the critical point known, it ought to give $A_\gamma/A_{\mathcal{T}} = 2$, at least if the finite volume effects can be avoided. This can be used as a stringent test for any theoretical calculation of the propagator near the critical point.

The ratio $A_\gamma/A_{\mathcal{T}}$ can also be measured in simulations of the full Ginzburg-Landau theory,³¹ and in principle also in superconductor experiments, since the vortex tension is related to the critical field strength by $H_{c1} = \mathcal{T}/2\pi$. We believe that such experiments would face the same difficulties in measuring the penetration depth as we did with the photon mass, but if a reliable measurement can be carried out, the ratio λ^{-1}/H_{c1} could be used to estimate how much closer to the critical point one would have to go to see the true scaling in the penetration depth. As in the experiments in Ref. 10, the penetration depth $\lambda = m_\gamma^{-1}$ we measured in our simulations was apparently obeying the mean-field scaling $\nu' = 1/2$, but it became consistent with the inverted XY behaviour $A_\gamma/A_{\mathcal{T}} = 2$ when $(\beta - \beta_c)/\beta_c \lesssim 0.002$.

Acknowledgements

We would like to thank K. Kajantie, H. Kleinert, M. Laine and D. Litim for useful discussions. AR was supported by PPARC and also in part by the ESF COSLAB programme and the National Science Foundation Grant No. PHY99-07949.

APPENDIX A: CURRENT CORRELATOR IN FREE-FIELD THEORY

In this appendix we derive Eq. (72) by assuming that the vortices are non-interacting free fields at the critical point. This means that the dual theory is simply a continuum theory of a free complex scalar field ϕ with mass $m = \mathcal{T}$.

The current operator $j_i(\mathbf{x})$ is defined as $j_i = \text{Im}\phi^* \partial_i \phi$. We want to calculate the current-current correlator $\langle j_i(-\mathbf{p}) j_j(\mathbf{p}) \rangle$. To do this, we write

$$j_i(\mathbf{p}) = \int d^3x e^{i\mathbf{p}\cdot\mathbf{x}} j_i(x) = -\frac{1}{2} \int \frac{d^3q}{(2\pi)^3} (2q_i + p_i) \phi^*(\mathbf{p} + \mathbf{q}) \phi(\mathbf{q}). \quad (\text{A1})$$

Then the correlator is

$$\langle j_i(\mathbf{p}) j_j(\mathbf{p}') \rangle = \frac{1}{4} \int \frac{d^3q}{(2\pi)^3} \frac{d^3r}{(2\pi)^3} (2q_i + p_i)(2r_j + p'_j) \langle \phi^*(\mathbf{p} + \mathbf{q}) \phi(\mathbf{q}) \phi^*(\mathbf{p}' + \mathbf{r}) \phi(\mathbf{r}) \rangle. \quad (\text{A2})$$

Assuming that the vortices do not interact, the expectation value factorizes,

$$\langle j_i(\mathbf{p}) j_j(\mathbf{p}') \rangle = \frac{1}{4} \int \frac{d^3q}{(2\pi)^3} \frac{d^3r}{(2\pi)^3} (2q_i + p_i)(2r_j + p'_j) \langle \phi^*(\mathbf{p} + \mathbf{q}) \phi(\mathbf{r}) \rangle \langle \phi^*(\mathbf{p}' + \mathbf{r}) \phi(\mathbf{q}) \rangle, \quad (\text{A3})$$

and using the tree-level propagator

$$\langle \phi^*(\mathbf{p})\phi(\mathbf{p}') \rangle = (2\pi)^3 \delta(\mathbf{p} - \mathbf{p}') \frac{1}{p^2 + m^2}, \quad (\text{A4})$$

we obtain the one-loop integral

$$\langle j_i(\mathbf{p})j_j(\mathbf{p}') \rangle = (2\pi)^3 \delta(\mathbf{p} + \mathbf{p}') \frac{1}{4} \int \frac{d^3q}{(2\pi)^3} \frac{(2q_i + p_i)(2q_j + p_j)}{(q^2 + m^2)((\mathbf{p} + \mathbf{q})^2 + m^2)}. \quad (\text{A5})$$

Now, this is a tensor that depends only on one vector \mathbf{p} , so it must be generally of the form

$$\langle j_i(-\mathbf{p})j_j(\mathbf{p}) \rangle = A(p) \left(\delta_{ij} - \frac{p_i p_j}{p^2} \right) + B(p) \frac{p_i p_j}{p^2}, \quad (\text{A6})$$

where $A(p)$ and $B(p)$ are functions of the absolute value of \mathbf{p} only. The duality in Eq. (35) implies that up to a constant multiplicative factor and with some constant C , the photon correlator is

$$\langle B_i(-\mathbf{p})B_j(\mathbf{p}) \rangle = \left[A(p) + C \right] \left(\delta_{ij} - \frac{p_i p_j}{p^2} \right) + \left[B(p) + C \right] \frac{p_i p_j}{p^2}. \quad (\text{A7})$$

Since we know that B_i is sourceless, we must have $B(p) = -C$, and it is straightforward to calculate its value

$$B(p) = \frac{p_i p_j}{p^2} \langle j_i(-\mathbf{p})j_j(\mathbf{p}) \rangle = \frac{1}{4p^2} \int \frac{d^3q}{(2\pi)^3} \frac{(2\mathbf{p} \cdot \mathbf{q} + p^2)^2}{(q^2 + m^2)((\mathbf{p} + \mathbf{q})^2 + m^2)} = -\frac{m}{8\pi}. \quad (\text{A8})$$

This means that the gauge field susceptibility $\chi_A(p)$ defined in Eq. (59) is

$$\chi_A(p) = \frac{1}{p_x^2 + p_y^2} \langle B_3(-\mathbf{p})B_3(\mathbf{p}) \rangle = \frac{1}{p_x^2 + p_y^2} \left(1 - \frac{p_z^2}{p^2} \right) \left[A(p) + \frac{m}{8\pi} \right] = \frac{1}{p^2} \left[A(p) + \frac{m}{8\pi} \right]. \quad (\text{A9})$$

We can calculate $A(p)$ by contracting $\langle j_i(-\mathbf{p})j_j(\mathbf{p}) \rangle$ with the transverse projection operator,

$$(D-1)A(p) = \frac{1}{p^2} \int \frac{d^3q}{(2\pi)^3} \frac{p^2 q^2 - (\mathbf{p} \cdot \mathbf{q})^2}{(q^2 + m^2)((\mathbf{p} + \mathbf{q})^2 + m^2)}, \quad (10)$$

and calculating the integral, we find

$$A(p) = -\frac{m}{16\pi} + \frac{p^2 - 4m^2}{32\pi p} \arctan \frac{p}{2m}, \quad (11)$$

and consequently

$$\chi_A(p) = \frac{1}{16\pi p^2} \left[m + \frac{p^2 - 4m^2}{2p} \arctan \frac{p}{2m} \right], \quad (12)$$

up to an overall constant factor, which we parameterize by c_A in Eq. (72). The value of m_γ , on the other hand, is fixed to $m_\gamma = 2m = 2T$.

* Electronic address: neuhaus@pcu.helsinki.fi

† Electronic address: a.k.rajantie@damtp.cam.ac.uk

‡ Electronic address: kari@nordita.dk

¹ M. E. Peskin, *Annals Phys.* **113**, 122 (1978).

² C. Dasgupta and B.I. Halperin, *Phys. Rev. Lett.* **47**, 1556 (1981).

³ A. Kovner, P. Kurzepa and B. Rosenstein, *Mod. Phys. Lett. A* **8**, 1343 (1993) [Erratum-ibid. *A* **8**, 2527 (1993)] [arXiv:hep-th/9303144].

⁴ M. Kiometzis, H. Kleinert and A. M. J. Schakel, *Phys. Rev. Lett.* **73**, 1975 (1994).

⁵ M. Kiometzis, H. Kleinert and A. M. J. Schakel, *Fortsch. Phys.* **43**, 697 (1995).

⁶ M. Hasenbusch and T. Török, arXiv:cond-mat/9904408.

⁷ D. S. Fisher, M. P. A. Fisher and D. A. Huse, *Phys. Rev.*

B43, 130 (1991).

⁸ I. F. Herbut and Z. Tesanovic, *Phys. Rev. Lett.* **76**, 4588 (1996) [arXiv:cond-mat/9605185].

⁹ S. Kamal, R. Liang, A. Hosseini, D. A. Bonn and W. N. Hardy, *Phys. Rev.* **B58**, R8933 (1998).

¹⁰ K. M. Paget, B. R. Boyce and T. R. Lemberger, *Phys. Rev.* **B59**, 6545 (1999).

¹¹ K. Kajantie, M. Laine, T. Neuhaus, A. Rajantie and K. Rummukainen, *Nucl. Phys. Proc. Suppl.* **106**, 959 (2002) [arXiv:hep-lat/0110062].

¹² P. R. Thomas and M. Stone, *Nucl. Phys. B* **144**, 513 (1978).

¹³ H. Kleinert, *Lett. Nuovo Cim.* **35**, 405 (1982).

¹⁴ P. Olsson and S. Teitel, *Phys. Rev. Lett.* **80**, 1964 (1998).

¹⁵ J. Hove and A. Sudbo, *Phys. Rev. Lett.* **84**, 3426 (2000).

- ¹⁶ T. Banks, R. Myerson and J. B. Kogut, Nucl. Phys. B **129**, 493 (1977).
- ¹⁷ R. Savit, Phys. Rev. B **17**, 1340 (1978).
- ¹⁸ J. Villain, J. Phys. (France) **36**, 581 (1975).
- ¹⁹ J. V. Jose, L. P. Kadanoff, S. Kirkpatrick and D. R. Nelson, Phys. Rev. B **16**, 1217 (1977).
- ²⁰ K. Kajantie, M. Laine, T. Neuhaus, J. Peisa, A. Rajantie and K. Rummukainen, Nucl. Phys. B **546**, 351 (1999) [arXiv:hep-ph/9809334].
- ²¹ A. V. Pochinsky, M. I. Polikarpov, B. N. Yurchenko, Phys. Lett. **A154**, 194 (1991).
- ²² A. Hulsebos, arXiv:hep-lat/9406016.
- ²³ A. K. Nguyen and A. Sudbo, Phys. Rev. **B60**, 15307 (1999).
- ²⁴ K. Kajantie, M. Laine, T. Neuhaus, A. Rajantie and K. Rummukainen, Phys. Lett. B **482**, 114 (2000) [arXiv:hep-lat/0003020].
- ²⁵ M.E. Fisher, M.N. Barber and D. Jasnow, Phys. Rev. **A8**, 1111 (1973).
- ²⁶ C. de Calan and F.S. Nogueira, Phys. Rev. **B60**, 4255 (1999).
- ²⁷ D. T. Son, JHEP **0202** (2002) 023 [arXiv:hep-ph/0201135].
- ²⁸ B. Bergerhoff, F. Freire, D. Litim, S. Lola and C. Wetterich, Phys. Rev. B **53**, 5734 (1996) [arXiv:hep-ph/9503334].
- ²⁹ R. H. Swendsen and J. S. Wang, Phys. Rev. Lett. **58**, 86 (1987).
- ³⁰ K. Binder, Rep. Prog. Phys. **50**, 783 (1987).
- ³¹ K. Kajantie, M. Laine, T. Neuhaus, A. Rajantie and K. Rummukainen, in progress.